Journal of Nano- and Electronic Physics
Vol. **13** No 1, 01007(6pp) (2021)

Журнал нано- та електронної фізики
Том **13** № 1, 01007(6cc) (2021)

A Theoretical Survey on the Potential Performance of a Perovskite Solar Cell Based on an Ultrathin Organic-Inorganic Electron Transporting Layer

B. Farhadi[1], F. Zabihi[2], Y. Zhou[1], A. Liu[1,*]

[1] *School of Physics, Dalian University of Technology, Dalian 116023, People's Republic of China*
[2] *State Key Laboratory for Modification of Chemical Fibers and Polymer Materials, Shanghai Belt & Road Joint Laboratory of Advanced Fibers and Low-dimension Materials, College of Materials Science and Engineering, Donghua University, Shanghai 201620, People's Republic of China*

(Received 30 December 2020; revised manuscript received 15 February 2021; published online 25 February 2021)

An ultrathin perovskite solar cell with 29.33 % theoretical power conversion efficiency (PCE) is designed for flexible applications. The perovskite layer is sandwiched between two multijunctions, i.e. poly(3-hexylthiophene) (P3HT), nickel oxide (NiO), and copper (I) thiocyanate (CuSCN) as the hole transporting element, from one side, and zinc oxide (ZnO), tin (IV) oxide (SnO_2) and phenyl-C61 butyric acid methyl ester (PCBM) as the electron transporting compartment, from the other side. This study uses a professional software package to accurately simulate a series of highly efficient perovskite-based solar cell structures that use both organic and inorganic materials. Calculations are simultaneously run with SCAPS (version. 3.3.07). The materials system for the electron transporting multijunction, bandgap of the perovskite layer, defection density, temperature of operating conditions, and concentration of charge doping are manipulated as the tuning parameters. An excellent fill factor (84.76 %), a potentially low entire thickness (~ 1 μm), and compatible nature for both organic and inorganic materials make this layout auspicious for a feasible and versatile high efficiency, but low-cost electronic devices. The constituent materials are selected based on the thickness and photoconversion efficiency. In order to assess the further potentials of materials system, we replaced CuSCN with PTAA (Polytriarylamine) and observed an increase in the theoretical efficiency, and we investigated the effect of varying the doping concentration in the PTAA layer. To simulate this structure, both the electrical and physical properties of the materials are considered, and the results are compared with those of previous works. These results should be of significant interest to experimentalists in the field.

Keywords: Perovskite solar cell, Electron transfer layer, Defect density, Temperature, Efficiency, Fill factor, SCAPS.

DOI: 10.21272/jnep.13(1).01007 PACS numbers: 05.45.Pq, 85.60.Bt

1. INTRODUCTION

Perovskite solar cells are known as the only alternatives for commercial silicon photovoltaic devices. Their speedy ramp-up from 2.2 % to 22 %, low-cost and availability promise a fascinating landscape toward a silicon-free market for solar energy in the near future [1, 2]. From both physical and manufacturing standpoints, perovskite materials are preferred for their tailorable composition and structure, their easily tunable bandgap, carrier mobility, charge density, diffusion length and optical parameters, which make them be simply designed in the form of ultrathin and flexible two dimensional energy packs [3, 4]. In a standard configuration, a perovskite solar cells are composed of five functional layers: a metal cathode, a hole-transporting layer (HTL), an active element (perovskite), an electron transporting layer (ETL), and an anode electrode. Perovskite layer absorbs the energy from incident photons, creates the excited electron-hole pairs, and in virtue of its bi-polar nature, conducts them to the corresponding electrodes, through the ETL and HTL Minutely, ETL extracts and transports electrons while blocking holes, and HTL selects and transports the holes and blocks the electrons [5, 6]. Based on such a simple concept, one may note that high electron mobility in the ETL and efficient hole mobility in the HTL crucially determine the efficiency of the photon-to-voltage conversion. The carrier mobility in charge selective layers is profoundly influenced by their electrical nature and a crystalline structure (lattice orientation and defection), as well as their bulk quality (uniformity, integrity, coverage and pin-hole density).

On the other hand, a smooth and immediate shuttling to and from the adjacent layers is strikingly determinant [7].

In the earliest stage of development of organic, inorganic perovskite materials, particularly $CH_3NH_3PbI_3$ demonstrated 2-3 % PCE. In a decade, in numerous efforts such as surfaces and interfaces engineering, lattice orientation design, architectural and compositional manipulations ended to a certified ~ 24 % photovoltaic function. While various structures and combination of materials system have been developed and compared, further controversies and ambiguities emerged and remained unsolved. As yet, a certain decision between the high-performance inorganic hole-electron transporting materials, e.g. titanium oxide (TiO_2), tin oxide (SnO_2), zinc oxide (ZnO), copper(I) thiocyanate (CuSCN) and nickel oxide (NiO), and their pliable and cost-effective organic counterparts, such as carbon allotropes, poly(3-hexylthiophene) (P_3HT) and poly(3,4-ethylene dioxythiophene) polystyrene sulfonate (PEDOT: PSS) is reckoned to be the most tedious engineer-

* aiminl@dlut.edu.cn

ing task. Besides, an inclusive design and in-depth theoretical surveys would lead us to select the *p*-i-*n* versus *n*-i-*p* stacking or the mesoporous versus the planar structure [8, 9].

Numerical modeling and simulation techniques allow foreseeing the results of the operational trails in a constrained domain of tuning factors and conditions. Our previous studies layout an optimized material system and configuration, yielding a high-performance, compatible, well-packed and long-lasting hybrid for both photon-harvesting and storage purposes [10].

In this work, we pursue with detail characterizations of ETL and HTL compartments, where their thickness, constituting materials and the quality of junction with perovskite layer are explicitly propounded. The most optimum projection resulted in an auspicious performance based on 29.33% PCE and 84.76% fill factor (FF), which are comparable with the highest theoretical reports. Use SCAPS in computation system reduces the risk of the drastic deviations respecting the experimental values. Beyond materials selection, different thicknesses and stacking alignment of functional layers are accounted and tested as the highly critical tuning metrics.

$CH_3NH_3PbI_3$ is adopted as the bone material for the photo-active element, and indium-tin-oxide (ITO) and Au are respectively accommodated as the front and back contacts. Such a popular choice avails facile analogies with the existing experimental results.

2. DEVICE STRUCTURE AND METHODOLOGY

The main goal of this numerical work is to suggest an idea configuration and materials system, for a perovskite, leading to the highest feasible power conversion efficiency and longer lifetime in a normal ageing and service condition. To this end, various functional materials and alignments are examined, while the overall thickness of the device is kept constant, at a minimum requirement.

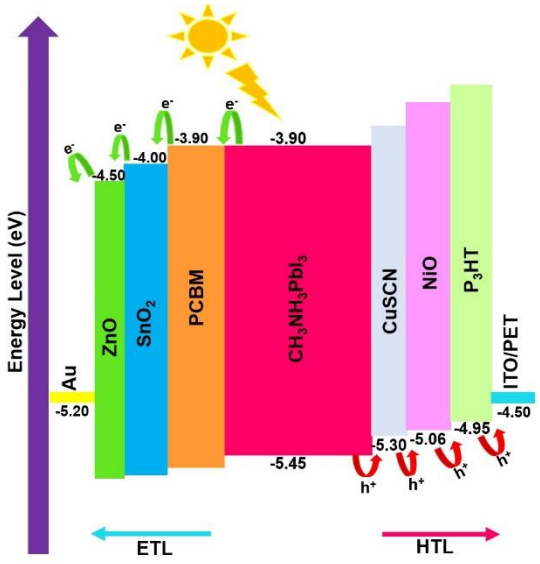

Fig. 1 – Energy diagram of perovskite multijunction

The energy levels and the profile of the energy in various functional junctions in the perovskite solar cells, simulated in this study, are depicted in Fig. 1. The energy levels in the materials are quantized, so the photons must be sufficiently energetic to excite the electrons to the higher levels.

The incident photons which their energy level is lower than that of the perovskite bandgap, pass through the cell rather than being absorbed by the active layer. Therefore, the bandgap engineering, via proper choices of materials system and junction alignment, would give the upper hand to the rate of carrier generation compared with recombination. On the other hand, the lifetime of the excited carrier must exceed the time, which is required to transfer the carriers from the lower to the high energy levels. One of the parasitic factors is the large offset between conduction bands of the active (perovskite) and the ETL, as of the same between the valance bands of HTL and perovskite. A large level of energy difference at the junctions creates and In this effort, we suggest a propitious approach (Figure 1), based on the use of the multiple ultrathin layers, with minor valance (conduction) energy differences, which collectively provide a smooth profile for a huge gradient.

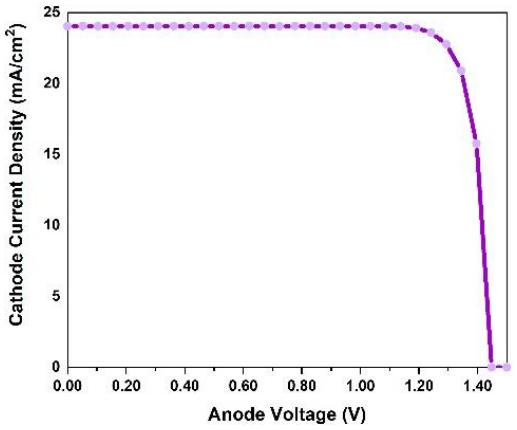

Fig. 2 – PV metrics calculated by SCAPS 1D simulation

Fig. 2 shows the *J*-*V* curve calculated based on a 400 nm thick perovskite layer, which is reckoned to be placed between P_3HT/NiO/CuSCN, multilayer as *p*-type and a PCBM/SnO_2/ZnO stacking layer as *n*-type. ITO and Au are considered as the front and rare contacts. Such an architecture, in theory, provides a 1.44 V open-circuit voltage (V_{oc}), a 23.93 mA/cm^2 current density (J_{sc}) and, with a 0.847 fill factor (FF), totally yielding 29.33 % PCE. This astonishing FF might be only achieved in theory, where the balk and microscopic impairs are unavoidably denied. In reality, however, the lattice imperfections and vacancies, the grain boundaries, the mismatch and gaps of the interfaces and the pin-hole created during crystallization and film formation all together act as the energy passivation and recombination sites. To make a batter overlap and reduce the deviation between theory and operation we rectify the calculation system by inserting the imperfection parameters, i.e. the boundary conditions at the interfaces of perovskite with carrier transporting layers [11, 12].

Fig. 3 presents the thickness diagram and the photovoltaic profile of the compact planar perovskite solar

cell, proposed in this study, where simulation was conducted in SCAPS 1D medium.

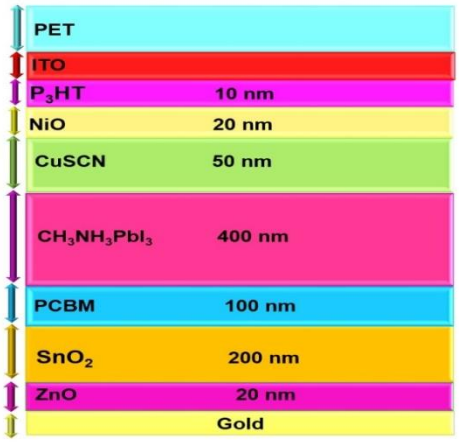

Fig. 3 – Thickness of individual layers of a planar perovskite solar cell simulated by SCAPS

2.1 Simulation Parameters

SCAPS is able to predict the PV behavior for a given geometry and alignment of a solar panel. Additionally, it allows users to select and optimize the most suitable materials, dimensions and orders of stacking for an electronic or optoelectronic device. For a unit or a module in the actual use, SCAPS detect and treat the operational risks. Design and prediction of parameters by SCAPS eliminate the expense and errors of experimentation and thus reduce the manufacturing cost. We use these software packages to design an ultrathin and flexible perovskite solar cell which in reality can be used as a part of wearable power packs.

3. RESULTS AND DISCUSSION

As a mean to pinpoint the influence of the defection density, the simulation runs were performed with different assumptions based on perfect and defective active layer and related interfaces. Moreover, the perovskite layer was replaced with various combinations, i.e. the organic-inorganic lead halide $CH_3NH_3PbI_3$ as well as the inorganic lead-free $CsSnI_3$ and $FASnI_3$. Further details on defections and thicknesses information will be presented in the optimization section. Fig. 3 depicts the proposed structure (from top to bottom), consisting PET/ITO as the anode contact, a 100 nm-P_3HT, a 200 nm-NiO and a 100 nm-CuSCN form a multijunction HTL. A 400 nm-$CH_3NH_3PbI_3$ perovskite layer was accommodated below, and a 100 nm-PCBM as ETL, a 200 nm-SnO_2 and a 100 nm-ZnO were contemplated to be serving as the ETL multijunction. Eventually, an Au thin film played the role of the rare contact [13, 14].

From a technical point of view, inorganic (organic) materials are preferred for being used as ETLs. This is simply due to their relative low unoccupied molecular orbital, desired work function, minor electron-injection barrier, superior electron mobility and hole blocking.

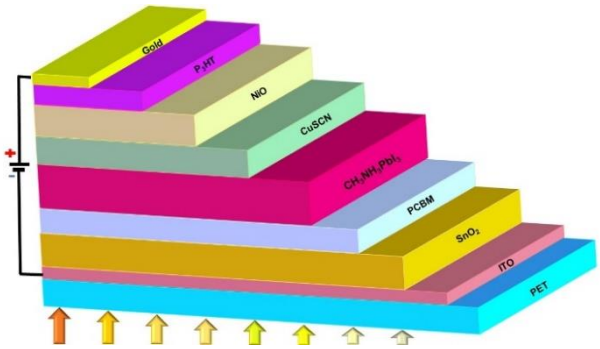

Fig. 4 – Compact and planar perovskite solar cell simulated by SCAPS 1D, based on organic-inorganic lead halide perovskite layer. Stacking model and circuit pathway

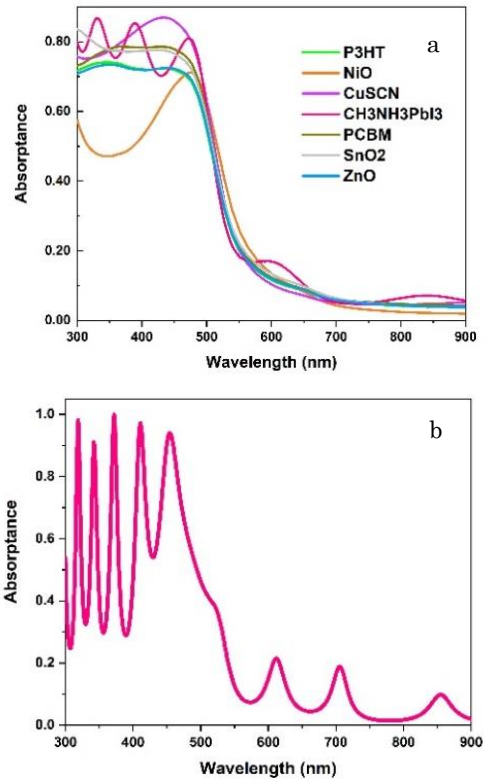

Fig. 5 – Compared light absorption profiles for different layers (a); Simulated light absorption in the visible range (b)

On the other hand, the inorganic semiconductors typically possess a high occupied molecular orbital, a low hole injection barrier, therefore make an extraordinary hole profile and electron buffer. Beyond their functional privilege, inorganic materials attenuate the chance of chemical interactions with the adjacent layers and last longer in the arduous service conditions. Semiconductive materials with an organic background, however, require inexpensive materials resources and manufacturing techniques, but their comparatively poor function and short life-time constrain their application. Here, we follow an approach of combination and synergy, as the heterojunctions of organic and inorganic materials are introduced for both hole and electron transporting layers (see Fig. 4). The layer is specific and depends on the nature of the material and the quality of the layer. Since the electrical potential is proportional to the series resistance, the theoretical

trend sounds principally in-line with what is expected in reality. The maximum electrical potential occurs at ITO/P_3HT interfaces, undertakes a trivial drop toward the inorganic p-type and perovskite layer, while follows an accelerated drop from PCBM/SnO_2 to the SnO_2/ZnO and the metal interfaces. This potential pathway, however, in theory, is formed because of the high doping distributions in n- and p-type layers, but it entirely approves the potential offsets between the adjacent layers, as shown in Fig. 1.

The theoretical light absorption profiles, compared for different layers, denotes that the absorption in visible range mainly takes places in the active layer. Nevertheless, the slight absorption of other organic and inorganic semi-conductive layers might be in reality due to some parasitic scattering and multiple internal reflections (Fig. 5). The incident absorption and visible absorptivity are applied to calculate the Quantum Efficiency (QE), which is an indication of the capability of the absorbed incident photons to create the electric current across a solar cell [15, 16]. It is defined by the ratio of the number of the charge carriers collected at the electrodes to the number of photons incident on the solar cell:

$$\mathrm{QE} = \frac{\mathrm{Electrons}_{\mathrm{out}}}{\mathrm{Photons}_{\mathrm{in}}} = \frac{J_{sc}/q}{p(\lambda)(hc/\lambda)}, \qquad (1)$$

where hc/λ is the energy of photons, λ is the wavelength, $p(\lambda)$ is the incident power as a function of λ, and q (> 0) is the charge of the generated electron.

3.1 Optimization of the Thickness of the Electron Transport Layer

The conduction band (valence band) edge of the ETL should be below that of the perovskite to extract electrons and block the holes. In addition, a functional ETL should be thin enough, allowing a smooth out-plane carrier motion, but be uniform and intact to minimize the chance for a short circuit. To meet these requirements, we tried a range of thicknesses, started from 100 nm, for the ETL, while fixed PCBM as the material candidate. The most favorable PCE is obtained by a 100 nm thick PCBM ETL, as demonstrated in Fig. 6a. Fig. 6b also show a similar trend when a SnO_2 thin film, varying from 200 to 500 nm, is employed as the ETL, where SnO_2 for a thickness. The maximum PCE has been approved when a 200 nm-SnO_2 layer is used for electron-transporting and hole blocking. Finally, with the same method of the simulation, the effect of thickness was tested for ZnO, ranging from 20 to 300 nm, as the best efficiency was registered for a 100 nm ZnO layer, comparatively as results are shown in Fig. 6c.

3.2 Effect of Polytriarylamine on the Proposed Structure

In order to assess the further potentials materials system, we replaced the CuSCN by a PTAA(Polytriarylamine) and observed an increase in theoretical efficiency to 29.36 %. By varying the doping concentration in the PTAA layer, as presented in Fig. 7, V_{oc} and PCE change proportionally.

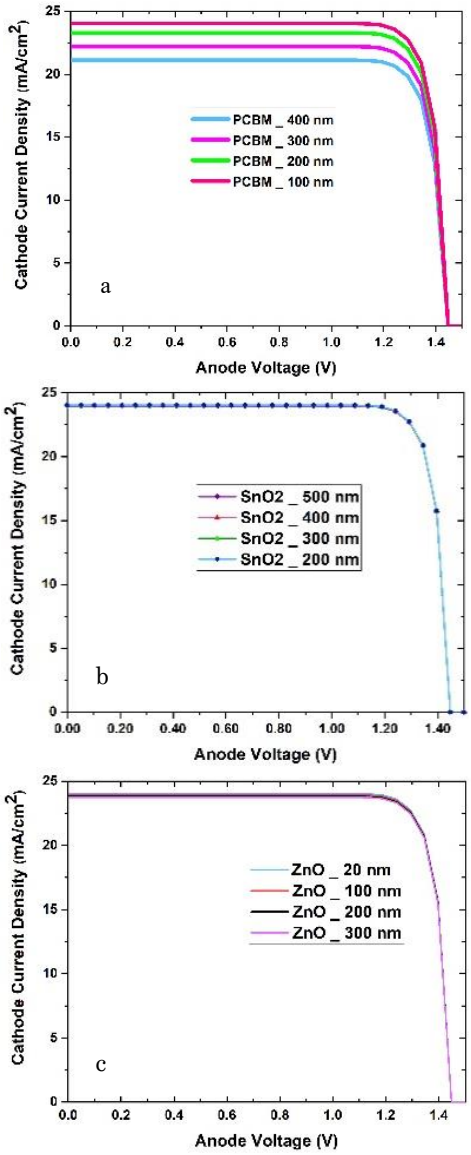

Fig. 6 – *J-V* curve for proposed structure for various PCBM thicknesses(a); *J-V* curve for proposed structure for various SnO_2 thicknesses(b); *J-V* curve for proposed structure for various ZnO thicknesses(c)

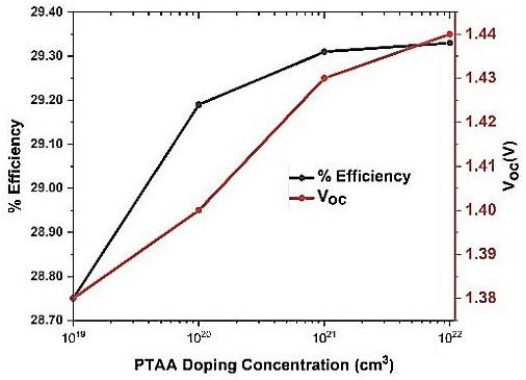

Fig. 7 – Photovoltaic behavior of simulated perovskite solar cell, versus doping concentration in PTAA, evolution V_{oc} and power conversion efficiency

3.3 Effect of Temperature on the Proposed Structure

The performance and stability of a perovskite solar cell are naturally susceptible to the temperature of the environment. There is also a serious concern about the accumulation of thermal energy during illumination. Fig.8 unveil that J_{sc} and V_{oc} unproportionally change with temperature and the best performance of temperature occurs at 300 K. The results also show that the efficiency decreases with increasing temperature, as expected.

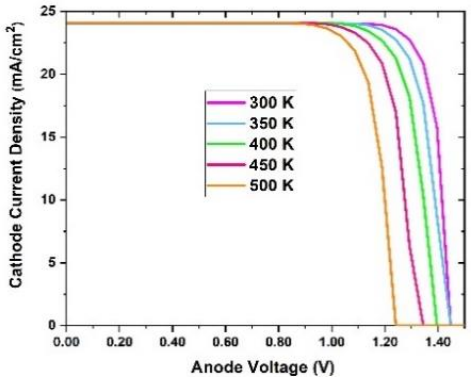

Fig. 8 – Effect of temperature on PV behavior of simulated perovskite solar cell, *J-V* curve

3.4 Effect of Perovskite Composition

Organic, inorganic and hybrid perovskites possess different physical, chemical and optic-electronic traits. Here, $CH_3NH_3PbI_3$, $CsSnI_3$ and $FASnI_3$ are investigated as the alternatives for perovskite materials (see Table 1, were respectively registered theoretical power conversion efficiencies of 29.33%, 29.02% and 28.49%, in optimum conditions.

Table 1 – Effect of perovskite composition on theoretical PV characteristics of the simulated solar cell

Material	V_{oc} (V)	J_{sc} (mA/cm²)	FF (%)	PCE (%)
$CH_3NH_3PbI_3$	1.44	23.93	84.76	29.33
$FASnI_3$	1.23	26.85	87.30	29.02
$CsSnI_3$	1.07	30.82	85.98	28.49

3.5 Effect of Defect Density in the Perovskite Layer

Shockley-Red-Hall recombination in CH3NH3PbI3 leads to a high defect density, N_t, which might predominately be due to the poor quality of functional films and interfaces. Shockley-Read-Hall recombination rate is theoretically expressed by Eqs. (2) and (3)

$$R_{SRH} = \frac{np - n_i^2}{\tau\left[p + n + 2n\cosh\left(\frac{E_i - E_t}{KT}\right)\right]}, \quad (2)$$

$$\tau = \frac{1}{\sigma N_t \upsilon_{th}}, \quad (3)$$

where τ is the carrier lifetime, N_t is the defect density, E_t is defect energy level, σ is the carrier capture, and υ_{th} is the carrier thermal velocity. The diffusion length of the carriers across the absorptive layer (L). Fig. 9 compare the structure with and without boundary conditions. In reality, the perovskite layer has relatively the highest density of defection, owing to a large number of lattice strains, lattice imperfection and grain boundaries.

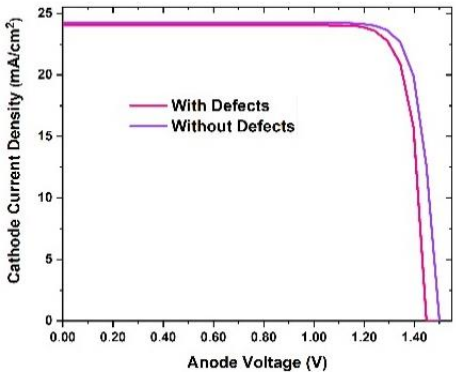

Fig. 9 – *J-V* curve with and without defects

Table 2 compares the PV parameters of the proposed structure, with those reported in some recent works. The proposed
structure offers improved performance in terms of efficiency and FF.

Table 2 – Comparison of solar cell parameters from this work with those of five recent simulations

Solar cell	V_{OC} (V)	J_{SC} (mA/cm²)	FF (%)	PCE (%)
Ref.[17]	1.08	25.33	79.27	21.64
Ref.[18]	0.92	22.56	76.74	14.03
Ref.[19]	1.15	23.34	70.31	18.92
Ref.[20]	1.24	23.77	87.96	26.11
This work	1.44	23.93	84.76	29.33

4. CONCLUSIONS

We use the SCAPS software to simulate perovskite solar cell structures. We vary thicknesses of the ETL materials to optimize efficiency. In addition, the efficiency of 29.33 % is obtained by using new materials. The advantage of this approach is not only that it considers electrical features in the simulation, but also that it applies physical features. The results are compared with and without the physical features. In the next step, we vary the defect density in the perovskite layer to determine the best efficiency, and we investigate how the operating temperature and bandgap affect the characteristics of the proposed perovskite structure. The proposed device is about 1 μm thick and is fabricated entirely from temperature-resistant materials.

This study obtains accurate results by using the SCAPS software packages, which allows us to investigate and optimize most of the important parameters that affect the electrical characteristics of perovskite solar cells.

REFERENCES

1. H.J. Snaith, *J. Phys. Chem. Lett.* **4**, No 21, 3623 (2013).
2. B. Farhadi, I. Marriam, S. Yang, H. Zhang, M. Tebyetekerwa, M. Zhu, S. Ramakrishna, R. Jose, F. Zabihi, *J. Power Source.* **422**, 196 (2019).
3. L. Zhao, D. Luo, J. Wu, Q. Hu, W. Zhang, K. Chen, T. Liu, Y. Liu, Y. Zhang, F. Liu, *Energ. Environ. Mater.* **4** No 1, 95 (2020).
4. H. Xiong, F. Zabihi, H. Wang, Q. Zhang, M. Eslamian, *Nanoscale* **10**, 8526 (2018).
5. A. Marchioro, J. Teuscher, D. Friedrich, M. Kunst, R. Van De Krol, T. Moehl, M. Grätzel, J. Moser, *Nat. Photon.* **8** No 3, 250 (2014).
6. Q. Li, A. Balilonda, A. Ali, R. Jose, F. Zabihi, S. Yang, S. Ramakrishna, M. Zhu, *Solar RRL* **4** No 9, 2000269 (2020).
7. N. Lakhdar, A. Hima, *Opt. Mater.* **99**, 109517 (2020).
8. M.I.H. Ansari, A. Qurashi, M.K. Nazeeruddin, *J. Photochem. Photobiol. C: Photochem. Rev.* **35**, 1 (2018).
9. F. Azri, A. Meftah, N. Sengouga, A. Meftah, *Sol. Energ.* **181**, 372 (2019).
10. Y. Raoui, H. Ez-Zahraouy, N. Tahiri, O. El Bounagui, S. Ahmad, S. Kazim, *Sol. Energ.* **193**, 948 (2019).
11. A.B. Coulibaly, S.O. Oyedele, B. Aka, *Model. Num. Simulat. Mater. Sci.* **9** No 4, 97 (2019).
12. W. Chang, H. Tian, G. Fang, D. Guo, Z. Wang, K. Zhao *Sol. Energ.* **186**, 323 (2019).
13. K. Chakraborty, M.G. Choudhury, S. Paul, *Sol. Energ.* **194**, 886 (2019).
14. M. Chowdhury, S. Shahahmadi, P. Chelvanathan, S. Tiong, N. Amin, K. Techato, N. Nuthammachot, T. Chowdhury, M. Suklueng, *Res. Phys.* **16**, 102839 (2020).
15. X. Zhang, F. Zabihi, H. Xiong, M. Eslamian, C. Hou, M. Zhu, H. Wang, Q. Zhang, *Chem. Eng. J.* **394**, 124887 (2020).
16. L. Lin, Jiang, P. Li, H. Xiong, Z. Kang, B. Fan, Y. Qiu, *Sol. Energ.* **198**, 454 (2020).
17. Q. Duan, J. Ji, X. Hong, Y. Fu, C. Wang, K. Zhou, X. Liu, H. Yang, Z-Y. Wang, *Sol. Energ.* **201**, 555 (2020).
18. S. Abdelaziz, A. Zekry, A. Shaker, M. Abouelatta, *Opt. Mater.* **101**, 109738 (2020).
19. S. Rai, B. Pandey, D. Dwivedi, *Opt. Mater.* **100**, 109631 (2020).
20. M.M. Salah, K.M. Hassan, M. Abouelatta, A. Shaker, *Optik* **178**, 958 (2019).